MODELLING TWISTED FLUX TUBES

PHILIP BRADSHAW (ASTROPHYSICS)

Abstract: Twisted flux tubes are important features in the Universe and are involved in the storage and release of magnetic energy. Therefore modelling the physical evolution of twisted flux tubes is a crucial step towards the understanding of basic physical phenomena in the Universe. In order to create a 3D model of twisted flux tubes, we model basic equations of electromagnetism based on a mathematical description from prescribed boundary conditions: the twisted flux tube is described as a cylinder on which the magnetic field is helically wrapped. The mathematical method is named magnetic field extrapolation. In this research exercise, two different methods were used: potential field and nonlinear force-free field. Both methods require prior knowledge of an analytical solution for the magnetic field that will be used as boundary conditions. Two scenarios were created: (i) a twisted flux tube with a constant radius and an increasing twist, and (ii) a twisted flux tube with a constant twist and an increasing radius. Within both scenarios, we study how the magnetic energy evolves and how each extrapolation method affects this evolution. Both increasing the twist and increasing the radius produced an exponential increase in magnetic energy: varying the twist producing an increase of 9.5%, and varying the radius producing an increase of 7.3%. While these results show that these numerical methods can be used to model twisted flux tubes, several key problems such as the limitations on the boundary conditions, especially the amount of twist which can be injected, must be addressed before further use of these modelling techniques.
Key words: Sun, Corona, Magnetic Fields, Flux Tubes, Numerical Methods, Simulation.

Introduction

A magnetic flux tube is a region of space forming a coherent structure that contains concentrated amounts of magnetic field: the flux tube is described by magnetic field lines which can be typically seen from the alignment of iron filings sprinkled on paper placed above a bar magnet. These field lines are such that the tangent at any point along the flux tube is in the same direction of the magnetic field itself. When the field lines are helically wrapped around the flux tube, the magnetic structure is called a twisted flux tube. Twisted flux tubes have been observed in many different environments in the Universe, such as the corona of the Sun (Régnier and Amari 2004), the torus formed by interaction between Jupiter's magnetosphere and one of its satellites, Io (Kivelson et al. 1997), and in Saturn's inner magnetosphere (André et al. 2007). Twisted flux tubes are also able to store and release large amounts of magnetic energy, due to the high concentration of magnetic field lines.

The physics of the solar structure is of particular interest for us. It is recognised that, when studying the Sun, flux tubes originate at the bottom of the convection zone in the interior of the Sun. It is in this region that the solar dynamo theory (Ossendrijver 2003) states that part of the global kinetic energy of the rotation of the Sun is transformed into magnetic energy; in other words, the poloidal magnetic field is converted into toroidal magnetic field by the differential rotation of the Sun's interior as described in Figure 1.

It is currently admitted (Hood et al. 2012) that a twisted flux tube formed near the convection zone becomes buoyant and thus starts to rise towards the surface of the Sun. When this twisted flux tube emerges through the solar surface, it can interact with already present magnetic fields. This interaction can cause solar events ranging from solar flares to Coronal Mass Ejections (Shibata et al. 1989). Because of their ubiquitous existence throughout the Sun and their implication in energetic phenomena, twisted flux tubes are of particular interest to many. The ability to understand the physics behind twisted flux tubes would greatly influence our current understanding of the Sun's atmosphere.

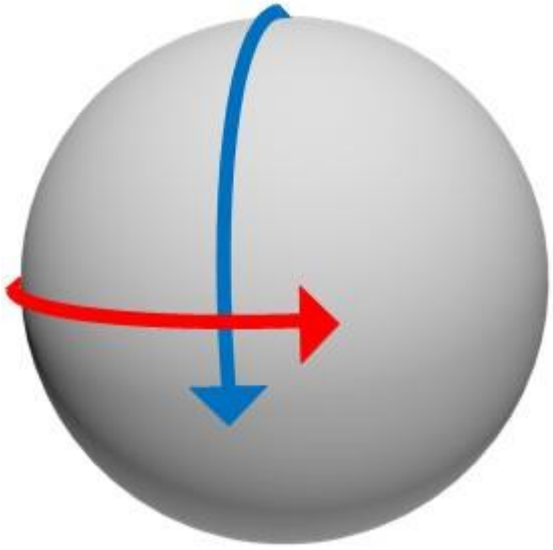

Figure 1 Shows a poloidal field (going down) and a toroidal field (going around)

Twisted flux tubes are magnetic in nature, and mostly localised in the corona. However, it is currently difficult to get accurate measurements of the magnetic field in the Sun's corona, and hence to determine the mechanism to store magnetic energy in the corona. This means that we have to get information on the magnetic field in other ways. The physical conditions (high density, low temperature) of the photosphere allow observers to easily measure the magnetic field at this level.

One common approach is to extrapolate the magnetic field through from the photosphere by considering the magnetohydrodynamic's force balance between the pressure exerted on the plasma (ionised gas), the force from the magnetic field, and the gravitational force,

$$-\nabla p + \mathbf{j} \times \mathbf{B} + \rho \mathbf{g} = \mathbf{0} \quad (1)$$

where *p* is the plasma pressure, *g* is the gravity, *ρ* is the density of the plasma, *j* is the electric current density, and *B* is the magnetic field within the flux tube.

This equilibrium arises when we consider the evolution of the magnetic structures that we are interested in are slower than the Alfvén speed, which corresponds to the speed at which the magnetic energy is transported along a magnetic field line (Dwivedi 2003). When considering a flux tube in the solar atmosphere (below 50 Mm height, say), we can ignore gravity as it is very small in relation to the variation of the magnetic field. Also if the plasma surrounding the flux tube has a low plasma β value (ratio of plasma pressure to magnetic pressure), then we can also neglect the plasma pressure forces: the corona plasma is dominated by the magnetic field. This reduces the equation down to simply $\times B = 0$. It is out of the above equation that our two extrapolation methods come from. If the electric current density is zero, so that

$$\nabla \times \mathbf{B} = \mathbf{0} \quad (2),$$

whilst also satisfying the equation

$$\nabla \cdot \mathbf{B} = \mathbf{0} \quad (3).$$

The magnetic field satisfying these two equations is known as a potential field. This assumption corresponds to a minimum of magnetic energy state and also assumes the field lines contain no twist. If, however, the electric current density is parallel to the magnetic field, in other words

$$\nabla \times \mathbf{B} = \alpha \mathbf{B} \quad (4)$$

where α is a function of position for the twist and sheer of the magnetic field lines, then this assumption is called the nonlinear force free field (NLFF). In addition, a NLFF field must also satisfy the equation

$$\mathbf{B} \cdot \nabla \alpha = 0 \quad (5)$$

which tells us that, while *α* can vary in space, it is a constant along each magnetic field line.

The potential and NLFF field are the two methods we used for simulating twisted flux tubes. For both methods, the normal component of the magnetic field needed to be stated on each boundary. The NLFF field also needs the twist of the field lines to be outlined on each boundary as well. We will describe in more details the boundary conditions in the next section.

Our aim during this research was to use numerical methods to simulate twisted flux tubes, and study how the magnetic energy is stored. Two different sets of simulations were run, one in which the radius of the flux tube was kept constant and increased the twist, and a second where the twist of the magnetic field lines was kept constant and the radius was increased. Both sets of simulations were set up by creating a Cartesian computational box (or data cube), and defining the normal component of the magnetic field vector as well as the twist of the magnetic field lines on each side boundary of the data cube. We used this numerical technique to mimic the twisted flux tubes observed in the solar atmosphere.

Method

1. Boundary Conditions

To solve the differential equations for each model mentioned above, we first need to define the boundary conditions (the magnetic field components that we have to impose on the sides of the computational box). In order to calculate the magnetic field and twist for each surface of the data cube, we used the analytical solutions found in Parker (1987). One thing that makes it simpler to create the needed boundary conditions is the fact that the tangent of the field lines in a flux tube must be in the same direction as the field itself. This means that, intrinsically, there is no radial component of the magnetic field of a flux tube. This simplifies our boundary conditions in that side boundary conditions for the magnetic field are zero. Therefore, only one component of the magnetic field B_z is needed for the top and bottom boundaries. However, the twist (α) must still be outlined for all boundary conditions. The analytical solutions describing a twisted flux tube in cylindrical coordinates were:

$$B_z(r) = B_0(1 + C^2\left(1-\frac{r^2}{R^2}\right)^4\left(1-\frac{6r^2}{R^2}\right))^2 \quad (6)$$

where B_0 is the external magnetic field strength, *R* is the radius of the flux tube and *C* is an arbitrary number defined so that solutions of B_z can be found, with $0 < C < \frac{9}{4}$. In addition, the twist can be written as:

$$\alpha(r) = \frac{2\times 5^{\frac{1}{2}}\times C(1-\frac{3r^2}{R^2})}{R[1+C^2\left(1-\frac{r^2}{R^2}\right)^4\left(1-\frac{6r^2}{R^2}\right)]^{\frac{1}{2}}} \times \left(1-\frac{r^2}{R^2}\right) \quad (7).$$

It should be noted that we have corrected the formula derived by Parker in order to ensure that the magnetic field is force-free. Using equations (6) and (7), we were able to set up our boundary conditions, and thus run our two modelling techniques.

Once both models where finished we then had to investigate the magnetic energy within the flux tubes. This was done by using the equation for magnetic energy:

$E = \int_V \frac{B^2}{2\mu_0} dV.$ (8).

From equation (8), we can not only calculate the magnetic energy within the system, but we can also calculate the free magnetic energy

$\Delta E = E_{NLFF} - E_{Pot}.$ (9).

As the potential field is a minimum of magnetic energy, the free magnetic energy is always positive. The free magnetic energy is an estimate of the amount of magnetic energy that can be released during an eruptive process. These two equations are the key ones that allow us to analyse the magnetic energy within our modelled flux tubes, but first we need to set up the models themselves.

2. Numerical Experiments

Before the boundary conditions could be assimilated into the numerical code, we first needed to convert equations (6) and (7) from cylindrical coordinates to Cartesian coordinates. The modified equations came out as:

$$B_z(r) = B_0 \left[1 + C^2 \left(1 - \frac{\left(x^2+y^2\right)^2}{R^2}\right)^4 \left(1 - \frac{6\left(x^2+y^2\right)^2}{R^2}\right)\right]^2 \quad (10)$$

$$\alpha(r) = \frac{2\times 5^{\frac{1}{2}} \times C\left(1-\frac{3(x^2+y^2)^2}{R^2}\right)}{R\left[1+C^2\left(1-\frac{(x^2+y^2)^2}{R^2}\right)^4\left(1-\frac{6(x^2+y^2)^2}{R^2}\right)\right]^{\frac{1}{2}}} \times \left(1 - \frac{(x^2+y^2)^2}{R^2}\right) \quad (11)$$

where B_0 is the external magnetic field strength, *R* is the radius of the flux tube and C is an arbitrary number, with $0 < C < 9/4$.

Using equations (10) and (11), each of the boundary conditions needed was created. The potential field computation needed only the vertical component of the magnetic field B_z, whilst the NLFF field computation needed both the vertical component of the magnetic field B_z and the twist α. Each boundary condition themselves are 100 pixels by 100 pixels making a computational box of 100 pixels cube.

We ran two different models: one where the twist varied by varying α, and another where the radius *R* varied. For both models, the constant B_0 was given a value of 1. For the variable twist model, a value of 30 was chosen for the radius (*R*) and an initial value of 0.1 was given for *C*, which would increase by 0.1 each time, until it reached a value of 2.2. For the variable radius model, a constant value of 1.5 was set for *C*. The radius began with a value of 12.5 and increased by 2.5 each time, until a value of 40 was reached. The quantities used in these models are dimensionless.

Results

Having successfully run the two sets of simulations, the first result from these experiments is that we were indeed successful in modelling both sets of twisted flux tubes: (i) one with a varying twist and (ii) another with a varying radius. In Figure 2 (a) and (b), we give an example of the computations carried out. We plot few magnetic field lines to outline the structure of the flux tube. In Figure 2 (a), the potential field model is shown: there is no twist and the magnetic field lines are straight. In Figure 2 (b), the NLFF model shows twisted magnetic field lines induced by the twist. In the NLFF model, even if the field lines are twisted, the flux tube is still well defined as a coherent structure.

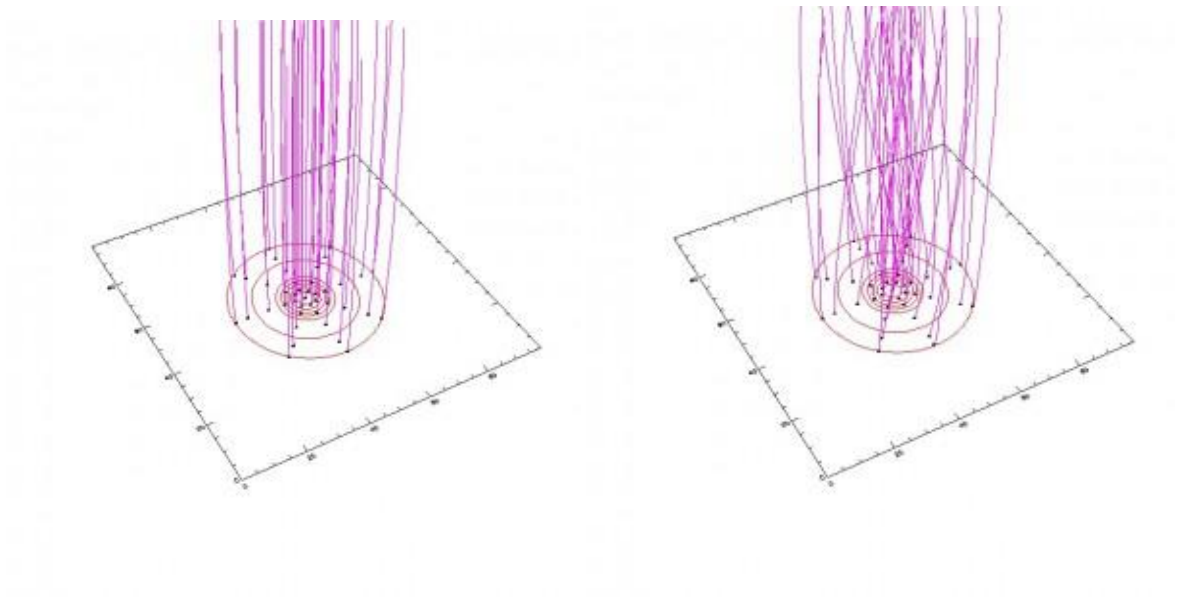

(a) (b)

Figure 2

2 (a) Potential field model; **2 (b)** Nonlinear force-free model exhibiting twisted field lines
The magnetic field forming the flux tube are plotted in pink. The contours represent the strength of the magnetic field with the flux tube)

When looking at how the magnetic energy and free magnetic energy evolved, for both cases four graphs where plotted. Figure 3 shows how the magnetic energy for the potential field and NLFF evolved with increasing *C* and how the free magnetic energy evolved with increasing *C*.

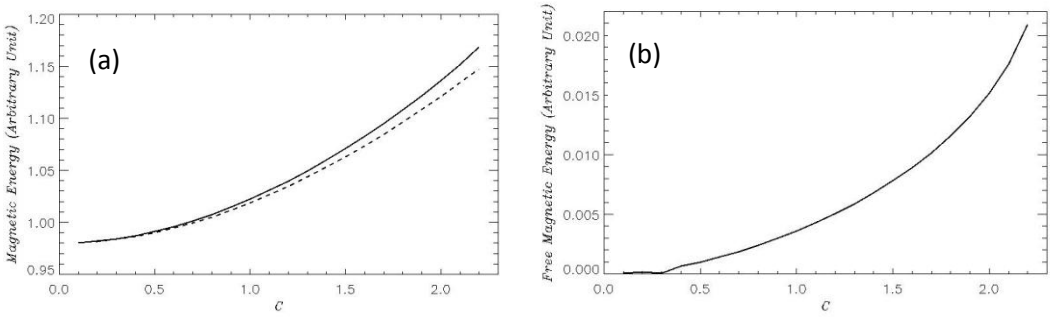

Figure 3

3 (a) Magnetic energy for the potential field (dashed line) and NLFF field (solid line) when varying the twist (C); **3 (b)** Free magnetic energy evolution as the twist (C) is increased.

Figure 4 shows how the magnetic energy for the potential field and NLFF evolved by increasing *R*, and how the free magnetic energy evolved by increasing *R*.

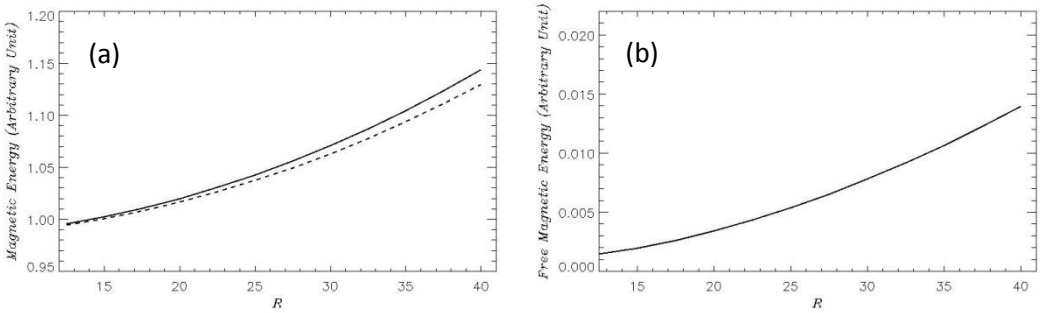

Figure 4

4 (a) Magnetic energy for the potential field (dashed line) and NLFF field (solid line) when varying the radius (R); **4 (b)** Free magnetic energy evolution as the radius (R) is increased.

Finally, Figure 5 shows logarithmic plots of the variation of magnetic energy for both an increasing value of *C* and an increasing value of *R* (NLLF field in solid line, potential field in dashed line).

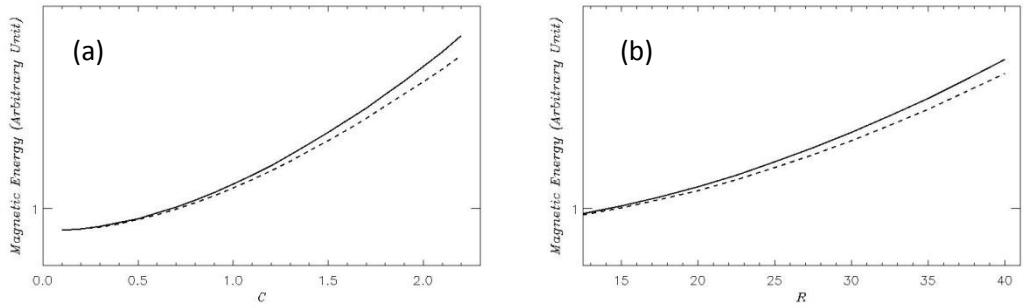

Figure 5 Log plots of the variation of magnetic energy

5 (a) Magnetic energy for the potential field (dashed line) and NLFF field (solid line) when varying the constant (C); **5 (b)** Magnetic energy for the potential field (dashed line) and NLFF field (solid line) when varying the radius (R)

Discussion

Whilst we were successful in simulating two different twisted flux tubes, there were several limitations in modelling flux tubes with this extrapolation technique. For instance, initially when attempting to model a flux tube with varying radius, we used a value of 10 for the radius and a *C* value of 1.5. It was found that the numerical code for the NLFF field did not converge (i.e., did not find an equilibrium state), and so we were unable to model a flux tube of that radius. This again shows that we are limited as to how we can model twisted flux tubes and that we can only get reliable results if we keep our models within certain conditions.

Additionally, we were only able to run our sets of models with a value of 1 for the external magnetic field (B_0). Since magnetic field within the flux tube depends on the external magnetic field (see equation (6)), different values of B_0 would significantly change the values of B_z.

The main part of this study was to investigate how the magnetic energy within that system evolves with increasing twist and radius. For the case of increasing twist, it can be seen that the two models were very similar up to a value of 0.5 for *C* (Figure 3 (a)). This can be explained by the fact that for the NLFF field, there is very little twist in the system due to the low value for *C*. This means that the magnetic field lines are still almost straight lines, which is precisely how the potential field models the magnetic field lines in this experiment. It can be seen that after *C* equals 0.5, the two models begin to differ significantly. For low values of twist the percentage difference between the two models was about 0.004%, and this increased to a difference of 1.8% for the highly twisted cases.

This is a large difference and it shows that, for highly twisted flux tubes, the potential field model is simply not accurate enough.

When we look at the shape of the lines themselves which exhibit a more pronounced spiral structure, we can see that after a value of 1 for *C*, the magnetic energy in both systems increased exponentially. This is also something we can also see when we look at the free magnetic energy in the system (Figure 3 (b)).We can test this hypothesis by looking at the log plot of the magnetic energy in Figure 5 (a). As we can see, both the NLFF (solid line) and the potential field (dashed line) can be approximated to a straight line, due to the fact that they both vary very little as the value of *C* is increased. Because they can both be approximated to straight lines, it means that both the NLFF and potential field increase exponentially as *C* is increased. Fitting a straight line to both sets of data gives us a slope of 0.05 for the NLFF field and a slope of 0.04 for the potential field. This supports our approximation that they are both straight lines in Figure 5, meaning that they both increase exponentially.

Another point to note is that when we look at the low twist in the free magnetic energy, we can see a small feature. This arises because the two models are so similar at very low twist that the difference will be very small and subject to the numerical errors in the code. Looking at the overall increase of magnetic energy, we see that the magnetic energy has increased by 9.5% from low twist to high twist. This is a noticeable increase for a flux tube that does not have a strong magnetic field.

When we look at how the magnetic energy evolves with increasing radius (Figure 4 (a)), we can see that the increase in magnetic energy is not as sharp. The slope is more smoothed out, showing that the twist of the field lines could have more of an effect on the magnetic energy than the radius of the flux tube itself. As before, this can be tested by looking at the log plot in Figure 5 (b), where we can see that the log of the magnetic energy increases by only a small amount, as the radius is increased. Fitting a straight line to the data gives us a slope of 0.03 for the NLFF field (solid line) and a slope of 0.02 for the potential field (dashed line). Both of these slopes are less than those found in the log plot for the variation of *C*, which indicates a variation in *C* produces a greater variation in magnetic energy, compared to a variation in the radius of the twisted flux tube. There is an intrinsic difference already between the two models. For increasing radius, it begins as a percentage difference of 0.14% and increases to 1.2%. This is mainly due to the value of *C* we used for the evolving radius. With a value of 1.5 for *C*, there is already some twist within the flux tube, meaning that the two models will not be as similar as those for lower twist.

Further investigation as to what value of *C* we choose when we are investigating increasing radius is something that may shed more light on how much of an effect the twist of the flux tube has on the magnetic energy due to increasing twist. Looking at the magnetic energy as a whole, we see an increase of 7.3%. This supports the idea that the twist of the field lines has more of an effect on the energy within the flux tube than the radius of the flux tube itself. Looking at the free magnetic energy for increasing radius, we see a similar increase in magnetic energy as with the free magnetic energy for increasing twist. However, there are some differences, such as Figure 4 (b), where the slope is more linear in shape than that seen in Figure 3 (b). We also do not see the numerical errors seen in Figure 3, due to the fact that there is already twist built into the model.

Conclusions

The results show that both of our extrapolation methods can successfully model twisted flux tubes. However, there are limitations as to the kind of flux tubes you can model and how much twist can be injected in the model. We also found that increasing twist causes the magnetic energy to increase by 9.5% and increasing radius caused the magnetic energy to increase by 7.3%. As noted, it appears that increasing the twist causes the magnetic energy to increase much more rapidly than increasing the radius. In both cases the free magnetic energy also increased, and again the free magnetic energy increased more for the case of increasing twist. For the case of increasing twist, it was shown that the two models (potential fields and NLFF fields) are very similar for low twist models, but gradually diverge with increasing twist. This was also seen in the case of increasing radius; however, there was an intrinsic difference due to twist already in the system. Several issues are still unresolved, such as how different values for the external magnetic field affect the simulations, or how much twist we have already in the case of increasing radius affects the outcome.

References

André, N., Persoon, A.M., Goldstein, J.,Burch, J.L., Louarn, P., Lewis, G.R., Rymer, A.M., Coates, A.J., Kurth, W.S., Sittler, E.C., Thomsen, M.F., Crary, F.J., Dougherty, M.K., Gurnett, D.A., Young, D.T. 2007. 'Magnetic signatures of plasma-depleted flux tubes in the Saturnian inner magnetosphere', *Geophysical Research Letters* 34, 14108-14114.

Dwivedi, B.N. 2003. *Dynamic Sun*. Cambridge: Cambridge University Press, 231.

Hood, A.W., Archontis, V., Mac Taggart, D. 2012.'3D MHD Flux Emergence Experiments: Idealised Models and Coronal Interactions', *Solar Physics* 278, 3-31.

Kivelson, M.G., Khurana, K.K., Russell, C.T., Walker, R.J. 1997. 'Intermittent short duration magnetic field anomalies in the Io torus, Evidence for plasma interchange', *Geophysical Research Letters* 24, 2127-2130.

Ossendrijver, M. 2003. 'The solar dynamo', *The Astronomy and Astrophysics review* 11, 287-367.

Parker, E.N. 1987. 'Magnetic reorientation and the spontaneous formation of tangential discontinuities in deformed magnetic fields', *The Astrophysical Journal* 2, 876-887.

Régnier, S, Amari, T. 2004. '3D magnetic configuration of the Hα filament and X-ray sigmoid in NOAA AR 8151', *Astronomy and Astrophysics* 425, 345-352.

Shibata, K., Tajima, T., Steinolfson, R.S., Matsumoto, R. 1989. 'Two-dimensional magnetohydrodynamic model of emerging magnetic flux in the solar atmosphere', *The Astrophysical Journal* 345, 584-596.